Molecular orbital coefficients and transition dipoles of real polyenes

Bryan E. Kohler, Lyuba I. Malysheva, and Alexander I. Onipko

Additional information on J. Chem. Phys.
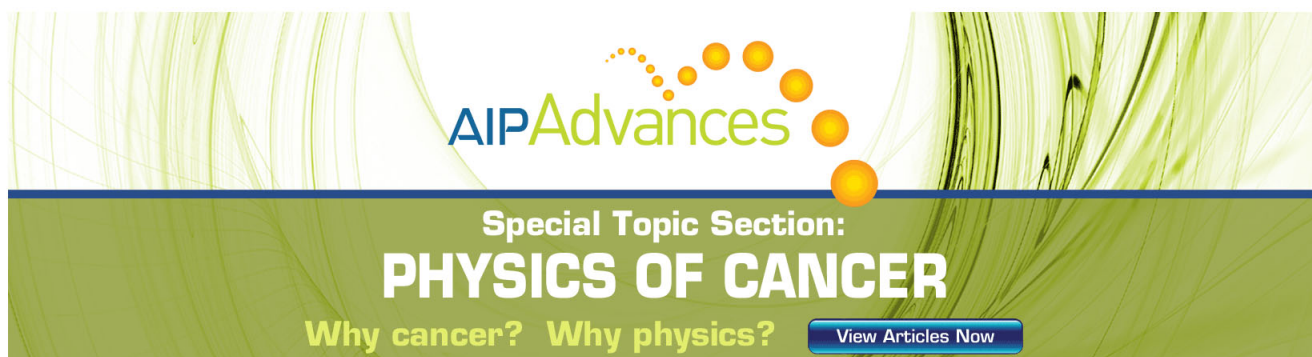
Molecular orbital coefficients and transition dipoles of real polyenes

Bryan E. Kohler
Department of Chemistry, University of California, Riverside, California 92521-0403

Lyuba I. Malysheva and Alexander I. Onipko
Bogolyubov Institute for Theoretical Physics, Kiev, 252143, Ukraine

A simple four configuration model that quantitatively reproduces all of the $1\,^1B_u$ and $2\,^1A_g$ state 0-0 energies that have been measured in high resolution spectroscopic experiments has been described previously. This model has been useful for explaining trends in the electronic properties of series of unsubstituted and substituted linear polyenes. While this model led to analytical expressions for the excitation energies, there were no closed form expressions for other quantities, such as the transition dipoles, that depend explicitly on the coefficients of the one-electron molecular orbitals. This paper derives exact expressions for the one-electron molecular orbital coefficients for an alternating chain as well as exact expressions for the transition dipole moments. This facilitates a detailed examination of the dependence of the transition dipole moments on the polyene length and alternation parameter which leads to an expression that accurately describes the dependence of the transition dipole moments on these chain parameters. The application of these expressions to an analytical analysis of nonlinear response in linear polyenes will be the subject of a subsequent paper. © *1995 American Institute of Physics.*

I. INTRODUCTION

It is well known that theory at the one-electron (Hartree–Fock) level fails to correctly order the first and second excited singlet states of linear polyenes and that correcting this failure requires explicit consideration of electron-electron interaction.[1] Because of the extensive delocalization and high correlation of the π electrons in linear polyenes, treatment of electron-electron interaction by configurational mixing must be carried to at least the double configuration interaction level. Exact calculations at this level for polyenes with three or four bonds in conjugation requires the use of supercomputers: for polyenes with more than eight double bonds they presently cannot be done. This unfortunate mismatch between our ability to measure electronic properties of linear polyenes (for example, nonlinear optical response) and our ability to provide correct microscopic interpretations generates a need for simple models that can quickly and reliably relate experimentally measured quantities to charge distributions in the relevant electronic states.

Such a model has already been proposed.[2] It is based on only four configurations: the ground configuration ($1\,^1A_g$ state) where all bonding molecular orbitals are doubly occupied; two configurations generated from the ground state by promoting one and two electrons from the highest energy occupied molecular orbital or HOMO to the lowest energy unoccupied molecular orbital or LUMO ($1\,^1B_u$ and A_g2 configurations, respectively); and the symmetric linear combination of two degenerate configurations which correspond to the promotion of an electron from the HOMO to the LUMO+1 and from the HOMO−1 to the LUMO (A_g3 state). This model only considers mixing of the A_g2 and A_g3 configurations which are treated empirically. The corresponding matrix element of the electron-electron repulsion operator is set equal to $A + B/N_d$, where N_d is the number of double bonds in the polyene chain, and the constants A and B are chosen to reproduce the experimentally measured excitation energies. Thus, the model is defined by these constants and the parameters of the one-electron Hamiltonian.

The success of this simple model in accounting for the S_1 and S_2 excitation energies of substituted and unsubstituted polyenes (see Ref. 3 for a review), raises the challenge of testing its ability to account for a wider variety of optical properties. Some numerical calculations of linear and nonlinear optical responses have already been reported,[4] but such calculations cannot provide the depth of insight into nonlinear optical response that would follow from an analytical description. The key step in obtaining this analytical description is the derivation of expressions for the transition dipole moments. Since the transition dipole moments are exquisitely sensitive to the details of how electrons are distributed along the polyene chain, such expressions would be extremely powerful tools.

In this paper we derive exact equations for the one-electron molecular orbital coefficients for an alternating polyene chain. These then lead to analytical expressions for all transition dipole moments. This is the decisive step towards constructing an analytical theory of nonlinear response in the framework of the model proposed in Ref. 2. We conclude with a detailed examination of the dependence of the HOMO-LUMO transition dipoles of neutral and ionic polyenes on the chain length and alternation parameter.

II. HAMILTONIAN, EIGENFUNCTIONS AND ENERGY SPECTRUM

A. Hamiltonian

The Hückel Hamiltonian is the simplest and most successfully parametrized one-electron Hamiltonian for describing the π-electron electronic structure of linear polyenes. It is employed here in a commonly used form with two parameters: the electron resonance transfer energy between the
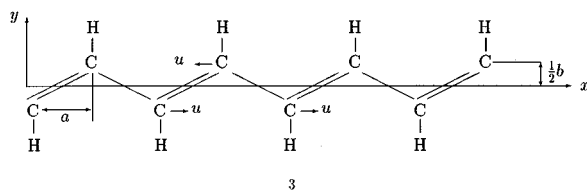
FIG. 1. Linear polyene segment with four double bonds. The correct bond alternating polyene geometry can be obtained by shifting each CH group from its position in an undimerized chain along the x-axis by u as shown by arrows. We have assumed a bond alternating geometry that mimics the structure of octatetraene (Ref. 6): C=C=1.332 Å, C—C=1.451 Å, $\angle$C=C—C=125°, so that a=1.235 Å, b=0.641 Å, and u=0.034 Å.
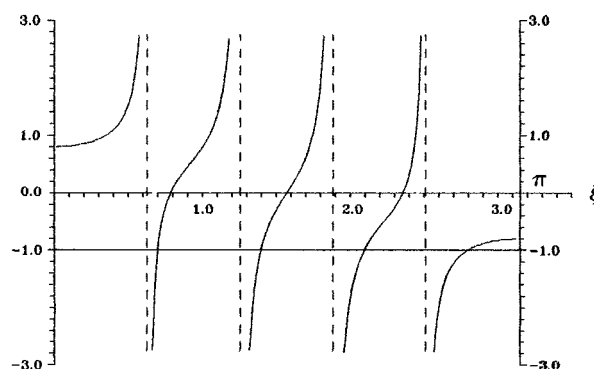

FIG. 2. Graphical solution to equation 12 for a linear polyene with four double bonds. Only the four first roots of this equation, determined by intersections of the horizontal line $(=-\exp 2\eta)$ with curves $\sin N_d\xi / \sin(N_d+1)\xi$ are shown. Just these roots numbered according to their magnitude are used in one-electron energy spectrum (14). For the case of $\eta=0$ and $N_d=4$ these roots are: $2\pi\mu/9$, where $\mu = 1, 2, 3$, and 4.

nearest-neighbor CH groups in an undimerized polyene t_0 $(t_0<0)$, and its change due to dimerization $\pm\kappa u$ expressed in terms of the electron-phonon coupling constant κ and the C–C-bond alternation u along the molecule axis,[5] see Fig. 1.

We start with the Hückel type electronic Hamiltonian for a terminated chain of N CH groups $(N=2N_d)$ connected by "single" and "double" bonds as shown in Fig. 1. In the tight-binding representation it has the form

$$H=\frac{1}{2}\sum_{j=1}^{N}((1-(-1)^j)[\beta_d|j\rangle\langle j+1|+(1-\delta_{j,1})\beta_s|j\rangle$$
$$\times\langle j-1|]+(1+(-1)^j)[(1-\delta_{j,N})\beta_s|j\rangle\langle j+1|+\beta_d|j\rangle$$
$$\times\langle j-1|]),\qquad(1)$$

where $|j\rangle\equiv c_j^+|0\rangle$, $|0\rangle$ is the vacuum wave function, c_j^+ and c_j are the Fermi operators which create and destroy π electrons of spin $\pm\frac{1}{2}$ on the jth CH group (electron spin variables are omitted for simplicity), β_s and β_d are the hopping integrals which determine the electron transfer energy between nearest neighbors connected by single and double bonds, respectively. It is implied in Eq. (1) that the stable polyene state corresponds to the chain with double bonds at its ends. We also assume that considering the ground and lowest excited states, σ electrons can be treated in the adiabatic approximation, i.e. that they contribute only to the vibrational part of the total Hamiltonian.

For the present analysis it is convenient to introduce instead of the hopping integrals new parameters

$$\beta_s=\beta\exp(-\eta),\quad\beta_d=\beta\exp\eta,\qquad(2)$$

which are related to parameters of the direct physical meaning by the simple equations

$$t_0=\beta\cosh\eta,\quad\kappa u=\beta\sinh\eta.\qquad(3)$$

B. Energy spectrum and wave functions

The solutions to the Schrödinger equation with the Hamiltonian H can be represented by the expansion

$$|\mu\rangle=\sum_{j=1}^{N}A_{j\mu}|j\rangle,\qquad(4)$$

where $A_{j\mu}$ is the jth component of eigenvector $\mathbf{A}_\mu$, $\mathbf{H}\mathbf{A}_\mu=E_\mu\mathbf{A}_\mu$, in the site representation; E_μ denotes eigenvalues of the H operator.

The eigenvector components can be found separately for the half spaces of odd $(j=2l-1, l=1,2,...,N_d)$ and even $(j=2l)$ chain sites. Denoting two corresponding vectors by $\mathbf{A}_\mu^{\text{odd}}$ and $\mathbf{A}_\mu^{\text{ev}}$, one easily gets, say, for the "odd half space"

$$(\mathbf{H}^0-\mathbf{V})\mathbf{A}_\mu^{\text{odd}}=\frac{E_\mu^2}{\beta^2}\mathbf{A}_\mu^{\text{odd}},\qquad(5)$$

where $N_d\times N_d$ matrixes $\mathbf{H}^0$ and $\mathbf{V}$ are defined by dimensionless operators

$$H^0=\sum_{l=1}^{N_d}[2|l\rangle\langle l|\cosh2\eta+(1-\delta_{l1})|l-1\rangle$$
$$\times\langle l|+(1-\delta_{lN_d})|l\rangle\langle l+1|],\qquad(6)$$

and

$$V=\delta_{ll'}\delta_{l1}|l\rangle\langle l'|\exp(-2\eta),\qquad(7)$$

respectively. The components of vector $\mathbf{A}_\mu^{\text{ev}}$ are connected with $\mathbf{A}_\mu^{\text{odd}}$ vector components by the simple relations

$$\frac{E_\mu}{\beta}A_{l\mu}^{\text{ev}}=(1-\delta_{lN_d})A_{l+1\,\mu}^{\text{odd}}\exp(-\eta)+A_{l\mu}^{\text{odd}}\exp\eta.\qquad(8)$$

The solution of Eq. (5) can be readily found by using the Lifshitz method.[7] Introducing the Green function operator $G=((E_\mu/\beta)^2-H^0)^{-1}$, Eq. (5) can be rewritten in the form of the Dison equation

$$\mathbf{A}_\mu^{\text{odd}}=-\mathbf{G}\mathbf{V}\mathbf{A}_\mu^{\text{odd}},\qquad(9)$$

or, equivalently,

$$A_{l\mu}^{\text{odd}}/A_{1\mu}^{\text{odd}}=-\langle l|G|1\rangle\exp(-2\eta),\qquad(10)$$

where the Green function matrix elements have been obtained in Ref. 8,

$\langle l|G|l'\rangle$

$$= \frac{2}{N_d+1} \sum_{k=1}^{N_d} \frac{\sin \frac{\pi k l}{N_d+1} \sin \frac{\pi k l'}{N_d+1}}{\left(\frac{E_\mu}{\beta}\right)^2 - 2\left(\cosh 2\eta + \cos \frac{\pi k}{N_d+1}\right)}. \tag{11}$$

The condition of nontrivial solvability of Eq. (10) can be written in the form

$$\langle 1|G|1\rangle = \frac{\sin N_d \xi}{\sin(N_d+1)\xi} = -\ \exp 2\eta \tag{12}$$

where the quantity ξ is related to eigenvalues of the Hamiltonian H by the following relation:

$$(E_\mu/\beta) = \pm \sqrt{2(\cos \xi + \cosh 2\eta)}. \tag{13}$$

According to Eqs. (12) and (13), N different eigenvalues of H are determined by N_d neighboring roots of Eq. (12) and by the choice of the sign in Eq. (13). We choose the first root as shown in Fig. 2 so that it corresponds to the lowest electron energy for the positive sign in Eq. (13) (β is negative). Then, using two indexes μ_v and μ_c for numbering the first positive N_d roots of Eq. (12), distinguishing the sign choice by indexes v (valence states or bonding molecular orbitals) and c (conduction states or antibonding molecular orbitals) we can write

$$E_{\mu_{v(c)}}^{v(c)} = -(+)2|\beta| \varepsilon_{\mu_{v(c)}}(\eta), \tag{14}$$

where $\varepsilon_{\mu_{v(c)}}(\eta) = 1/\sqrt{2} \sqrt{\cos \xi_{\mu_{v(c)}} + \cosh 2\eta}$. Note that $\mu_v = 1$ and $\mu_c = 1$ correspond to the lowest v state energy and to the highest c state energy, respectively, whereas $\mu_{v(c)} = N_d$ represents the reversed case.

Equations (8), (10), (12), and the normalization condition completely determine the components of the eigenvectors $\mathbf{A}_{\mu_v}^v$ and $\mathbf{A}_{\mu_c}^c$ which take the form

$$A_{j\mu_{v(c)}}^{v(c)} = \left(\frac{2 \sin \xi_{\mu_{v(c)}}}{(N+1)\sin \xi_{\mu_{v(c)}} - \sin(N+1)\xi_{\mu_{v(c)}}} \right)^{1/2}$$

$$\times \begin{cases} (-1)^{\mu_{v(c)}+1} \sin \frac{N+1-j}{2} \xi_{\mu_{v(c)}}, \\ j = 2l-1, \\ +(-)\sin \frac{j}{2} \xi_{\mu_{v(c)}}, \quad j = 2l, \end{cases} \tag{15}$$

where $\mu_{v(c)} = 1, 2, \ldots, N_d$. The phase in Eq. (15) is chosen so that

$$A_{j\mu_v}^v \rightarrow \sqrt{\frac{2}{N+1}} \sin \frac{\pi \mu_v j}{N+1}$$

and

$$A_{j\mu_c}^c \rightarrow \sqrt{\frac{2}{N+1}} \sin \frac{\pi(N+1-\mu_c)j}{N+1}$$

as $\eta \rightarrow 0$.

Thus, the diagonal form of the Hamiltonian for a finite polyene with alternating bonds reads

$$H = -2|\beta|\left(\sum_{\mu_v=1}^{N_d} \varepsilon_{\mu_v}(\eta)|\mu_v\rangle\langle\mu_v| \right.$$
$$\left. - \sum_{\mu_c=1}^{N_d} \varepsilon_{\mu_c}(\eta)|\mu_c\rangle\langle\mu_c| \right). \tag{16}$$

The eigenstates of this Hamiltonian (or the Hückel molecular orbitals for the polyene molecule) are

$$|\mu_{v(c)}\rangle = \sum_{j=1}^N A_{j\mu_{v(c)}}^{v(c)}|j\rangle, \tag{17}$$

where coefficients $A_{j\mu_{v(c)}}^{v(c)}$ are defined in Eq. (15).

The coordinate parts of the orbitals referred to in Sec. I. correspond to the choice in Eq. (17) of $A_{jN_d}^v$ and $A_{jN_d-1}^v$ for the HOMO and HOMO-1, and of $A_{jN_d}^c$ and $A_{jN_d-1}^c$ for the LUMO and LUMO+1, respectively. This is the case of the neutral polyene denoted as P. In the ionic forms of polyene with $2N_d-2$ (P^{++}) and $2N_d+2$ (P^{--}) π electrons on $2N_d$ carbon atoms, the highest occupied level in the ground state of P^{++} and P^{--} corresponds to $\mu_v = N_d-1$ and $\mu_c = N_d$, respectively. So, the HOMO and LUMO for P^{++} are the HOMO-1 and HOMO defined above for P. Similarly, the HOMO and LUMO for P^{--} are the LUMO and LUMO+1 for P.

III. TRANSITION DIPOLES

A. General case

The intensity of an optical transition depends on the transition dipole, the expectation value of the dipole moment operator between the initial and final states. In the case of transitions from the ground state (assumed to correspond to the single configuration where all valence states are doubly occupied) nonzero values only exist for excited state configurations that correspond to lifting an electron from one of N_d filled states μ_v to one of N_d empty states μ_c. If we assume that the π electron atomic orbitals of different C atoms do not overlap, the transition dipole moment $\mathbf{M}_{\mu_v \rightarrow \mu_c}$ expressed in units of ea (e—the absolute value of the electron charge, a—the distance along the chain axis between the nearest-neighbor carbon atoms in an undimerized chain, see Fig. 1) is given by the sum

$$\mathbf{M}_{\mu_v \rightarrow \mu_c} = -\langle\mu_c|\left(\sum_{j=1}^N \mathbf{r}_j|j\rangle\langle j| \right)|\mu_v\rangle. \tag{18}$$

The vector $a\mathbf{r}_j = (x_j y_j)$ determines the position of the jth C atom in the Cartensian coordinates, and the one-electron molecular wave functions $|\mu_{v(c)}\rangle$ are defined in Eqs. (15), (17). We use coordinates with the x-axis directed along the

molecular axis as shown in Fig. 1, so that y coordinates of C atoms are equal to $\pm b/2$. The C$=$C and C—C bond lengths were set to 1.332 Å and 1.451 Å, respectively, and all C$=$C—C bond angles were set to 125°.[6] With this choice we have for parameters shown in Fig. 1: $a=1.235$ Å, $b=0.641$ Å, and $u=0.034$ Å.

In terms of $\mathbf{A}^{v(c)}_{\mu_{v(c)}}$ vector components defined in Eq. (15), Eq. (18) can be rewritten in the form

$$M_{x\mu_v\to\mu_c} = -\left(\sum_{j=1}^{N}(jA^v_{j\mu_v}A^c_{j\mu_c}) + \frac{u}{a}\,\delta_{\mu_v\mu_c}\right), \qquad (19)$$
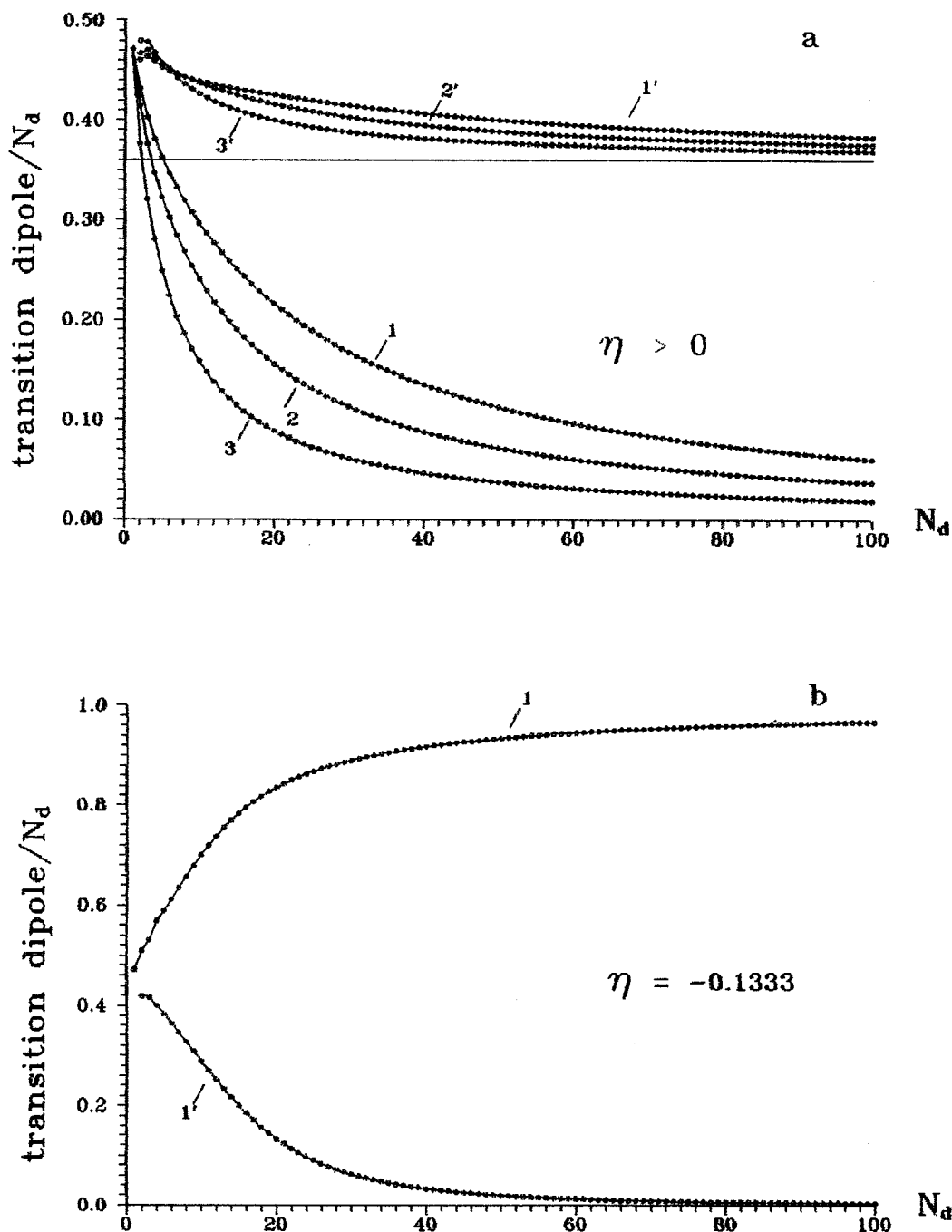

FIG. 3. HOMO–LUMO transition dipoles (in units of ea) per double bond in neutral and dicationic forms of alternating polyenes. **a**—curves 1, 2, and 3 represent $|M_x|/N_d$ calculated for $\eta=$ 0.08, 0.1333, and 0.2666, respectively; the correspondence between curves $1'$, $2'$, $3'$ and values of $|M_x^{++}|/N_d$ is the same; $\lim_{N\to\infty}|M_x^{++}|/N_d=2^5/(3\pi)^2\approx0.36$ is indicated by the horizontal line. **b**—curves 1 and $1'$ represent $|M_x|/N_d$ and $|M_x^{++}|/N_d$, respectively, for $\eta=-0.1333$.

$$M_{y\mu_v \to \mu_c} = \frac{b}{2a} \, \delta_{\mu_v \mu_c}, \qquad (20)$$

where we use the identity $\Sigma_{l=1}^{N_d} A_{2l-1\,\mu_v}^v A_{2l-1\,\mu_c}^c = -\Sigma_{l=1}^{N_d} A_{2l\mu_v}^v A_{2l\mu_c}^c = \frac{1}{2}\delta_{\mu_v\mu_c}.$

Substituting in Eq. (19) explicit expressions for $A_{j\mu_{v(c)}}^{v(c)}$ one obtains

$$M_{x\mu_v \to \mu_c} = \frac{1}{2} \frac{\exp 2\eta + \frac{1}{2}(N-1)\sinh 2\eta - \varepsilon_\mu^2(\eta)}{(N+1)\varepsilon_\mu^2(\eta) + \frac{1}{2}\sinh 2\eta} - \frac{u}{a}, \qquad (21)$$

for $\mu_v = \mu_c = \mu$ and

$$M_{x\mu_v \to \mu_c} = \frac{1+(-1)^{\mu_v+\mu_c}}{4} \frac{\sin \xi_{\mu_v} \sin \xi_{\mu_c}}{(\varepsilon_{\mu_v}(\eta) + \varepsilon_{\mu_c}(\eta))^2}$$

$$\times \frac{1}{\sqrt{(N+1)\varepsilon_{\mu_v}^2(\eta) + \frac{1}{2}\sinh 2\eta}}$$

$$\times \frac{1}{\sqrt{(N+1)\varepsilon_{\mu_c}^2(\eta) + \frac{1}{2}\sinh 2\eta}}, \qquad (22)$$

for $\mu_v \neq \mu_c$. In sum over states formalisms for calculating nonlinear optical response intraband transition dipole matrix elements are also needed. In the valence band (transitions between bonding molecular orbitals) these are

$$M_{x\mu_v \to \mu_v'} = \frac{1-(-1)^{\mu_v+\mu_v'}}{4} \frac{\sin \xi_{\mu_v} \sin \xi_{\mu_v'}}{(\varepsilon_{\mu_v}(\eta) - \varepsilon_{\mu_v'}(\eta))^2}$$

$$\times \frac{1}{\sqrt{(N+1)\varepsilon_{\mu_v}^2(\eta) + \frac{1}{2}\sinh 2\eta}}$$

$$\times \frac{1}{\sqrt{(N+1)\varepsilon_{\mu_v'}^2(\eta) + \frac{1}{2}\sinh 2\eta}}. \qquad (23)$$

The expression for $M_{x\mu_c \to \mu_c'}$ is the same.

Equations (21)–(23) determine exact dependences of the transition dipole moments on the chain length and alternation parameter. To get a transition dipole moment, one has to find the μ_vth and μ_cth roots of Eq. (12) for particular values of N and η and to use them together with the corresponding values of ε_{μ_v} and ε_{μ_c} in Eqs. (21), (22) or (23). Thus, provided that N, η, and $\varepsilon_{\mu_{v(c)}}$ are known, the relations given above immediately yield the transition dipole values which otherwise require computer calculations which become very lengthy for longer polyene chains.

Note that the calculated values of $|\mathbf{M}_{\mu_v \to \mu_c}|$ for the HOMO–LUMO transition in polyenes with three and four double bonds are (in debye): 7.064 and 8.595, respectively. These values (obtained for a slightly different geometry from that used throughout the rest of this paper, namely: C=C =1.34 Å, C—C=1.46 Å, $\angle$C=C—C=120°)[9] are in excellent agreement with those calculated for this geometry using much more elaborate theoretical methods which give 7.285 and 8.694.[9]

For an undimerized chain the above equations reduce to

$$M_{x\mu_v \to \mu_c} = \frac{1}{N+1} \begin{cases} (1+(-1)^{\mu_v+\mu_c}) \dfrac{\sin\dfrac{\pi\mu_v}{N+1} \sin\dfrac{\pi\mu_c}{N+1}}{\left(\cos\dfrac{\pi\mu_v}{N+1} + \cos\dfrac{\pi\mu_c}{N+1}\right)^2}, \\[4ex] (1-(-1)^{\mu_v+\mu_v'}) \dfrac{\sin\dfrac{\pi\mu_v}{N+1} \sin\dfrac{\pi\mu_v'}{N+1}}{\left(\cos\dfrac{\pi\mu_v}{N+1} - \cos\dfrac{\pi\mu_v'}{N+1}\right)^2}, \quad \mu_c = \mu_v'. \end{cases} \qquad (24)$$

B. HOMO–LUMO transitions

As seen from expressions (21)–(23), the value of the transition dipole depends sensitively on the chain parameters N and η, the type of the transition (interband or intraband) and the level indexes. In this section, we focus our attention on the HOMO-LUMO transitions for P and P^{++} which are of prime interest for comparison with experiment.

In accordance with its definition, the x-component of the HOMO-LUMO transition dipole in P takes the form (Eq. (21) with $\mu = N_d$, level indexes are omitted for simplicity)

$$M_x + \frac{u}{a} = \frac{1}{2} \frac{\exp 2\eta + N \sinh 2\eta - \cos \xi_{N_d}}{(N+1)(\cos \xi_{N_d} + \cosh 2\eta) + \sinh 2\eta}$$

$$= \begin{cases} 4N_d \pi^{-2}, & |\eta|N \ll 1, \\[1ex] (2\eta)^{-1}, & \eta N \gg 1, \ \eta > 0, \\[1ex] N_d, & |\eta|N \ll 1, \ \eta < 0. \end{cases} \qquad (25)$$

The analogous quantity for P^{++}, i.e., M_x^{++} (which is equal to M_x^{--}) is (Eq. (23) with $\mu_v = N_d - 1$, $\mu'_v = N_d$)

$$M_x^{++} = \frac{2\sin\xi_{N_d}\sin\xi_{N_d-1}(\sqrt{\cos\xi_{N_d}+\cosh 2\eta}-\sqrt{\cos\xi_{N_d-1}+\cosh 2\eta})^{-2}}{\sqrt{(N+1)(\cos\xi_{N_d}+\cosh 2\eta)+\sinh 2\eta}\sqrt{(N+1)(\cos\xi_{N_d-1}+\cosh 2\eta)+\sinh 2\eta}}$$

$$= \begin{cases} 4N_d\pi^{-2}, & |\eta|N \ll 1, \\ 32N_d(3\pi)^{-2}, & \eta N \gg 1,\ \eta > 0, \\ \pi 2^{-1/2}N_d^{-3/2}\eta^{-5/2}, & |\eta|N \gg 1,\ \eta < 0. \end{cases} \tag{26}$$
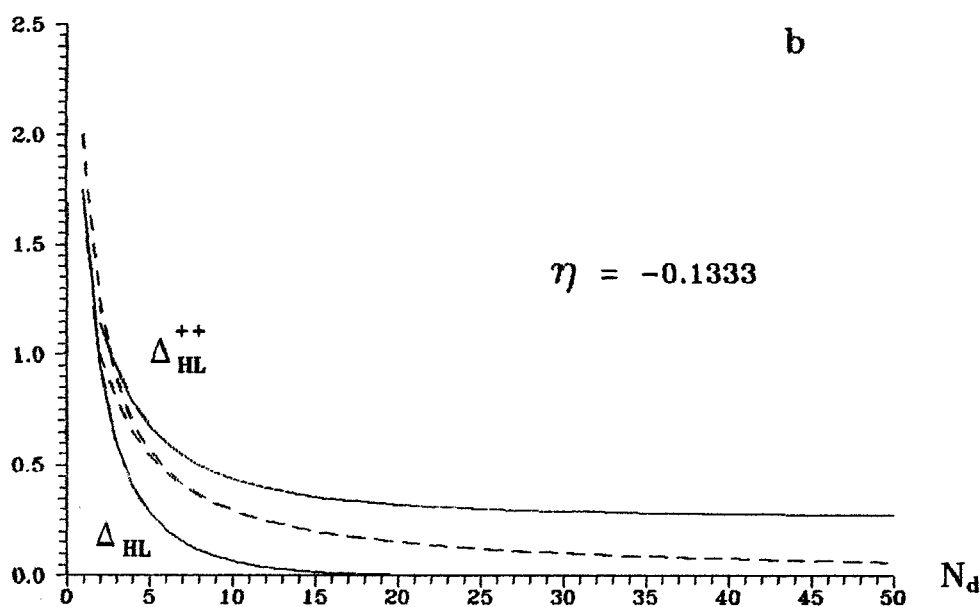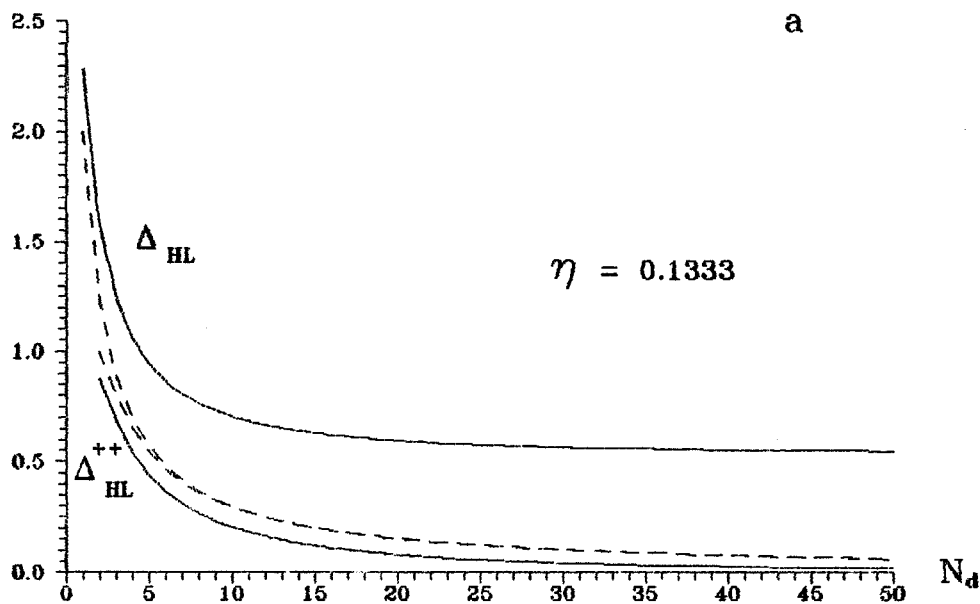

FIG. 4. HOMO-LUMO gap (in units of $|\beta|$) vs N_d in P (Δ_{HL}) and P^{++} (Δ_{HL}^{++}). Solid lines correspond to $\eta = 0.1333$ (a) and $\eta = -0.1333$ (b), dashed lines to $\eta = 0$.

Along with exact relations for M_x and M_x^{++}, we give in Eqs. (25), (26) the limiting expressions for transition dipoles found for long chains and small alternation ($N \gg 1$, $|\eta| \ll 1$) under the conditions $|\eta|N \ll 1$ and $|\eta|N \gg 1$. These expressions clearly show the qualitative difference in the behavior of M_x and M_x^{++} and the dramatic dependence of these quantities on the sign of η.

Consider first the case $\eta > 0$. We see that alternation strongly suppresses the transition dipole in P but it has a comparatively small effect on M_x^{++}, Fig. 3a. The maximal increase of M_x with the increase of the chain length is attained in the region of the intermediate asymptotics, $\eta N \ll 1$, where $M_x/N_d = 4\pi^{-2}$ (which is the true asymptotics in the undimerized chain). However, in reality the increase of M_x with N in the alternating chain is always less than proportional to N, and when $N \to \infty$, the dipole transition M_x saturates at the value $(2\eta)^{-1} - u/a$. At the same time, Eq. (26) says that $M_x \sim N$ if $N \gg 1$ and either $\eta N \ll 1$ or $\eta N \gg 1$. Since when $\eta N \gg 1$ the rate of increase of M_x^{++} with N is lower than when $\eta N \ll 1$, it can be concluded without calculations that the transition dipole per double bond in P^{++} decreases as the chain length increases whenever $N \gg 1$. Figure 3a shows the dependences $|M_x(N_d)|/N_d$ and $|M_x^{++}(N_d)|/N_d$ for some representative values of the alternation parameter. For moderate values of η (of the order of 0.2) the function $|M_x^{++}(N_d)|/N_d$ has a weak maximum at $N_d = 3$.

The linear response is determined by the oscillator strength of the HOMO-LUMO transition defined as $F_{HL} = F_0 \Delta_{HL} |M_x|^2$ (correspondingly, $F_{HL}^{++} = F_0 \Delta_{HL}^{++} |M_x^{++}|^2$), where Δ_{HL} (Δ_{HL}^{++}) is the HOMO-LUMO gap (in units of $|\beta|$) and $F_0 = 2m_e|\beta|a^2\hbar^{-2}$. Since Δ_{HL} for a neutral polyene tends to the constant value of 4η as $N \to \infty$ (see Fig. 4a),

whereas $\Delta_{HL}^{++} \sim N^{-2}n^{-1}$ in the same limit, the oscillator strength in P and P^{++} (F_{HL} and F_{HL}^{++}) turn out to be nearly equal (in contrast to the dipole transitions M_x and M_x^{++}). Figure 5 (curves 1 and 1') reproduces the dependence of the oscillator strength on the number of double bonds calculated for $\eta = 0.1333$. It is work emphasizing that the bond length alternation strongly supresses the intensity of linear absorption in long chains. Indeed, the maximum value of the oscillator strength F_{HL}^{max} ($\approx F_{HL}^{max\ ++}$) attained as $N \to \infty$ is approximately equal to $\eta^{-1}F_0$. For the typical polyene parameters $\eta = 0.1333$, $\beta = -30305$ cm^{-1}, $a = 1.235$ Å, $F_{HL}^{max} \approx 11$, whereas for the undimerized chain model the oscillator strength in this limit is proportional to the chain length: $\lim_{N \to \infty} F_{HL} = \lim_{N \to \infty} F_{NL}^{++} = 16\pi^{-3}N_dF_0$.

We turn now to the case $\eta < 0$. As seen from Eq. (12), under the condition $2|\eta| > \ln(N_d + 1)/N_d$ two states appear in the gap between valence and conduction states, which are placed symmetrically above and below the zero energy. This leads to radical changes in the N_d-dependence of both transition dipoles M_x and M_x^{++} (compare corresponding curves in Figs. 3a and 3b). The asymptotic behavior of the HOMO-LUMO gap in P and P^{++} also changes: Δ_{HL} goes to zero exponentially as $N \to \infty$, and $\lim_{N \to \infty} \Delta_{HL}^{++} = 2|\eta|$. As a result, the oscillator strength of the HOMO-LUMO transition at negative values of η is strongly suppressed in long chains, $|\eta|N \gg 1$: $F_{HL} \sim N^2 \exp(-|\eta|N)$, $F_{HL}^{++} \sim N^{-3}$ (see curves 2 and 2' in Fig. 5).

Thus, alternation produces significant effects on transition dipoles and hence, on optical properties only in long chains $|\eta|N > 1$. These effects are qualitatively different for the HOMO-LUMO transitions in neutral and doubly ionized polyene forms. Though distinctions between the behavior of
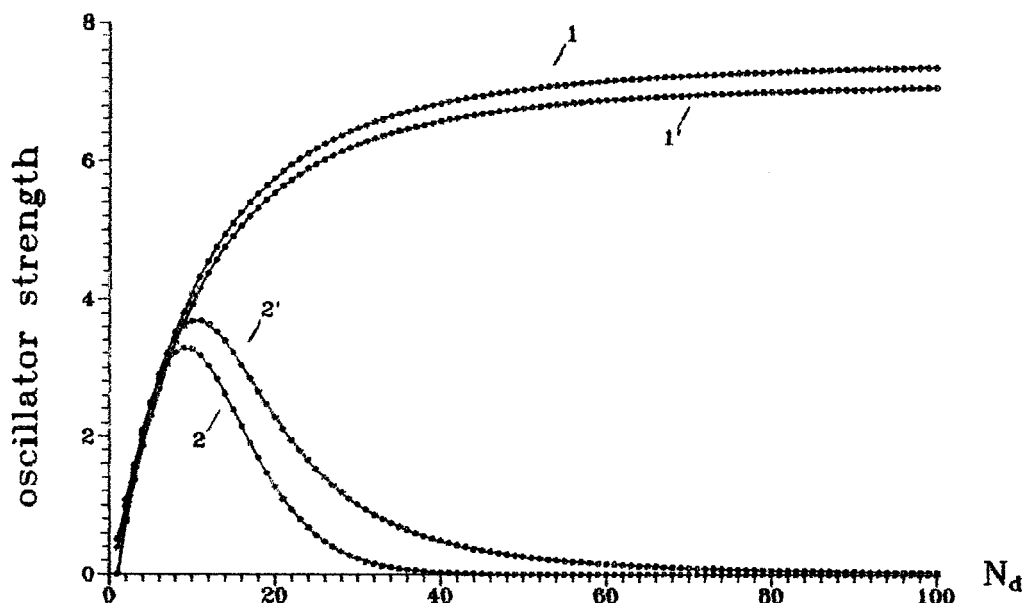

FIG. 5. Oscillator strength of the HOMO–LUMO transition polarized along the polyene axis in units of $F_0 = 2m_e|\beta|a^2\hbar^{-2}$: curves 1 and 2 represent F_{HL}/F_0 for $\eta = 0.1333$ and $\eta = -0.1333$, respectively; same is the correspondence between curves 2, 2' and values of F_{HL}^{++}/F_0.

M_x and M_x^{++} (which represent interband and intraband transition dipoles, respectively) are concealed in the linear absorption, they can be revealed by using data on the HOMO-LUMO gap dependence on the chain length which are readily available.

IV. CONCLUSION

A compact closed form of the Hückel molecular orbitals for real polyenes, which is nearly as simple as that for the chain without alternation, has been derived. The expressions for the Hückel molecular orbital coefficients obtained previously in Ref. 10 are seemingly equivalent but have a more complex structure that does not favor practical applications.

The central result of this paper is exact analytical expressions for all transition dipoles in polyenes, which relate the dipole transition values to the polyene length, alternation parameter, and energy of levels participating in the transition. This provides an extremely efficient tool for studying the optical response of polyenes. Here, as an example, we have examined the effect of alternation on the HOMO-LUMO linear absorption of neutral and ionized polyenes. The non-linear optical response is of immediate interest for the application of analytical results derived above. This work is currently in progress.

[1] D. Baersiwyl, D. K. Campbell, and S. Mazumdar, in *Conducting Polymers*, edited by H. Kiess (Springer-Verlag, Berlin, 1990).
[2] B. E. Kohler, J. Chem. Phys. **93**, 5838 (1990).
[3] B. E. Kohler, in *Conjugated Polymers*, edited by J. L. Bredas and R. Silbey (Kluwer, Dordrecht, 1991).
[4] J. K. Duchowski and B. E. Kohler, Mol. Cryst. Liq. Cryst. **256**, 449 (1994).
[5] W. P. Su, J. R. Schrieffer, and Heeger, Phys. Rev. B **22**, 1099 (1980).
[6] R. H. Baughman, B. E. Kohler, I. J. Levy, and C. Spangler, Synth. Metals **11**, 37 (1985).
[7] I. M. Lifshitz, Zh. Eksp. Teor. Fiz. **17**, 1017 (1947).
[8] K. Lakatos-Linderberg, R. P. Hemenger, and R. M. Pearlstein, J. Chem. Phys. **56**, 4852 (1972).
[9] K. Schulten and M. Karplus, Chem. Phys. Lett. **14**, 305 (1972).
[10] P. Karadakov, O. Castaño, F. Fratev, and V. Enchev, Chem. Phys. Lett. **78**, 560 (1981).